Proceedings of Global Power and Propulsion Society
ISSN-Nr: 2504-4400
GPPS Xi'an21
18th – 20th October, 2021
www.gpps.global

GPPS-TC-2021-231

EFFECTS OF LOCAL BLOCKAGE ON FILM COOLING EFFECTIVENESS OF A FAN-SHAPED HOLE FED BY CROSSFLOW

Pengmin L
University of Shanghai for Science and Technology
2274767434@qq.com
Shanghai, China

Xiaofeng C
University of Shanghai for Science and Technology
cxfusst@163.com
Shanghai, China

Chixiang L
University of Shanghai for Science and Technology
lcx_usst@163.com
Shanghai, China

Ren D
University of Shanghai for Science and Technology
dairen@usst.edu.cn
Shanghai, China

ABSTRACT

Effects of local blockage in the hole on film cooling effectiveness were investigated. The film cooling effectiveness (FCE) and heat transfer coefficient (HTC) of a fan-shaped hole was measured on a test rig of a flat plate with secondary crossflow in the coolant feeding passage. The blowing ratio was varied from 1 to 2 with a crossflow-to-mainstream momentum ratio of 0.4 and a blocking ratio of the hole was 25%. Results have revealed the difference of blockage effects at different locations. The blockage at the entrance side (Entr-side) and expansion side (Exp-side) walls concentrate the jet stream on one side, thus reducing the FCE values. Blockage on the laidback wall (Exp-back)slows down coolant velocity, leading to an accelerated dissipation of the film layer. The FCE values decrease as the blowing ratio is raised in the Entr-side case. The Blockage of Entr-side and Exp-back increased the heat transfer coefficient compared to the no blockage condition(clean), but the blockage on the diffuser side wall reduced the heat transfer coefficient compared to the clean condition. The heat transfer coefficient ratio of all holes increases with the increase of the blowing ratio. Results are indicative to evaluate the performance uncertainty of a fan-shaped hole in a real operating environment.

Keywords: film cooling effectiveness; blockage; fan-shaped hole; heat transfer coefficient; crossflow

INTRODUCTION

Film cooling is an important cooling technology to protect the gas turbine blades of modern advanced gas turbines. Coolant ejected from the blade internal channel adheres to the blade surface to form a thin layer of relatively low-temperature coolant which prevents the heat transfer from the hot gas to the blade metal surface. Aerojet engine ingests small ash and sandy particles from the atmosphere. Particles are likely to enter the coolant feeding passage and deposit in the film hole. The blockage in a film hole raises the local blade surface temperature and deteriorates the metal environment inside the turbine (Walsh et al.,2014).

There are many possible film hole blockages. The blockage location and size affect the film cooling effectiveness (FCE) value. Bunker (2000) investigated the influence of the exit blockage of round and fan-shaped film holes. Results reveal that in the case of thermal barrier coating blockage of 0.75mm thickness, a fan-shaped hole has much better tolerance than a round hole, although the cooling effectiveness of both holes is reduced. Lee et al. (2018) optimized the robustness of a film hole under the conditions of blockage and roughness. Results show that blockage has the dominant impact on the cooling efficiency of a film hole, and the primary feature of the optimization hole is the enlarged exit area.

Blockage at a specific place may augment the cooling effectiveness. Jovanovic et al. (2008) study the influence of blockage position on the film cooling efficiency of a round hole and found improved cooling effectiveness by the blockage at the outlet, especially at high-velocity ratios. Chen et al. (2021) used Large Eddy Simulation modeling to investigate the

effect of blockage at the outlet of a film hole and found similar results. All blockages reduce the flow rate coefficient but a blockage at the exit's front edge increases the film cooling efficiency (Huang et al.,2018). It was explained that the blockage at the exit front edge restrained the coolant to penetrate the mainstream, therefore the cooling efficiency is superior to other results.

A few valuable studies have been published on the blockage effect on film cooling holes with quantitative conclusions, but most results were obtained under hypothetical experiment conditions and are not credible (Bunker,2005). One critical condition is the entrance effect of secondary flow which is usually ignored and replaced by a coolant feeding plenum. The crossflow entrance is the normal coolant feeding way in turbine blades. Under the condition of crossflow coolant supply, the flow in a film hole is a complicated swirling one. The distribution of cooling efficiency downstream the hole is skewed to one side of the surface, which is significantly different from the condition of plenum supply (Kohli et al.,1998; Saumweber et al.,2008; Wilkes et al.,2016). It is of practical significance to investigate the blockage effect with the fed crossflow. While the effects of both blocked holes and crossflow have been studied before, there are no existing open-literature studies that examine the effect of blockage under internal crossflow conditions.

Experiments are carried out to investigate the influence of the local fixed blockages inside a fan-shaped film cooling hole. A specifically pyramid-shaped element is used to simulate the in-hole blockage for different blowing ratios and various blockage positions. The experimental setup, data processing method, and uncertainties are described in section two. The experimental results and discussion are presented in section three. The purpose of this work is to understand the blockage effects on film cooling effectiveness and heat transfer characteristics, which can provide not only a basis for the design scheme to counter this adverse effect but also a reference to judge the deterioration of cooling performance caused by the blockage in the actual operation of gas turbines.

EXPERIMENTAL METHOD

Experiment Setup

A fan-shaped film hole with a crossflow feeding is used to investigate the blocking effect on the FCE and HTC. The experiment layout is shown in Fig. 1, which has two flow paths to simulate the mainstream channel for high-temperature gas flow and the crossflow channel for internal coolant flow. The momentum ratio of secondary crossflow to the mainstream is 0.4. Both flows are air flows of different temperatures with a density ratio close to 1.0. The mainstream is blown into the test section through a convergent nozzle. The inlet turbulence intensity measured by a hotwire anemometer is less than 1%. The coolant flow rate is controlled by two mass flowmeters.

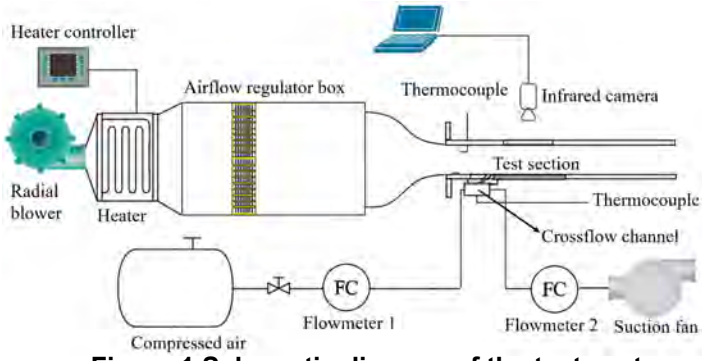

Figure 1 Schematic diagram of the test system

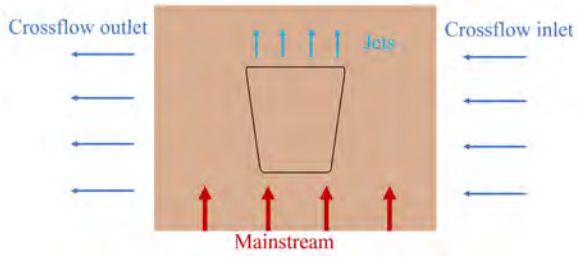

Figure 2 test bench chematic diagram

The mainstream channel has a quadrate cross-section of 100mm ×100mm with an 800mm length. the hole's inlet cylinder diameter D=7.2mm. A rectangular region of 10D×17D behind the hole's trailing edge is black painted for infrared radiation (IR) temperature measurement. Two Thermocouple is set at mainstream and crossflow channel to measure the temperature of hot air and coolant. In the FCE measurement, the channel bottom is made of a polymeric methyl methacrylate plate of thermal conductivity 0.17W /m/K. In the HTC measurement, an electrically heated Kapton sheet is attached to the back of a 0.2mm copper foil and is underlay with a fiberglass pad of 0.042 W /m/ K for thermal insulation. At the two ends of the crossflow channel, there are two mass flow rate meters to control a specified film blowing ratio. Fig. 2 shows the schematic diagram of the test bench.

A normal fan-shaped hole is used as the baseline hole model referred to as the clean hole in this study. The hole has an ejection angle of 35 deg with a lateral expansion angle of 10 deg and a laidback of 10 deg. It has a relatively large length diameter ratio of 12. It is a scaled-up hole to have a diameter of 7.2mm diameter of inlet round pipe with a length of 4.6 times its diameter.

Accurate prediction of blockage locations is another complex problem that is out of the present research reported in this paper. Three holes geometries with pyramid-shaped blockage are considered representative cases. The first one is on the inlet round pipe wall and named the Entr-side blockage. The second one is on the hole's laidback wall and named the Exp-back one. The third one is on the diffuser sidewall and is named the Exp-side. The blockage elements with the top

point at the center of the local cross-section of the film hole and the maximum local blocking ratio of 25%. The position of the blockage elements in the axial direction of the hole is determined by the distance between the top point of the blockage elements to the hole entrance. The Entr-side blockage element is located 1.5D from the entrance, which of Exp-back and Exp-side are 8D. The shape and size of blockage elements are determined by the two angles of the pyramid-shaped elements in the axial and radial direction of the hole. The detailed parameters are as shown in Fig.3.

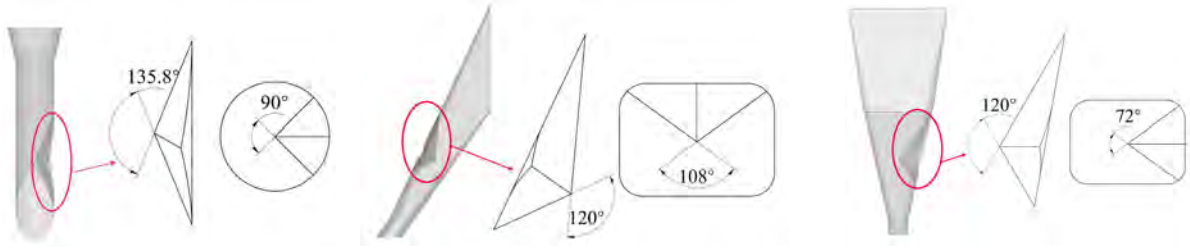

Entr-side Exp-back Exp-side

Figure 3 Configuration parameter of the blockages

In the FCE experiments, the mainstream velocity is maintained at 15m/s which is measured by a pitot probe 100mm ahead of the hole outlet. The mainstream Reynolds number with hole diameter as characteristic length is about 6000. The mainstream temperature was kept at 47±1℃, and the secondary flow temperature is 22℃ which were measured by K-type thermocouples embedded in the corresponding flows. In the HTC experiments, both temperatures of mainstream and secondary flow are 27℃. The power of the electrically heated Kapton sheet is 32.2w, in which the radiant heat exchange is about 2.38w. For both experiments, the blowing ratio (BR) is the difference value of flowmeter 1 and 2 and is controlled at BR =1.0, 1.5, and 2.0 respectively.

Data Processing Method

The BR is defined as:

$$BR = \frac{\rho_h U_h}{\rho_\infty U_\infty} = \frac{(m_{in} - m_{out}) / A_h}{\rho_\infty U_\infty} . \quad (1)$$

The adiabatic film cooling effectiveness is defined as:

$$\eta_{ad} = \frac{T_\infty - T_w}{T_\infty - T_c} . \quad (2)$$

HTC value represents the heat transfer capacity between the wall surface and the mainstream. HTC is defined as:

$$h = \frac{q}{T_\infty - T_w} . \quad (3)$$

The heat flux q is the ratio of electric heating power to the copper plate area. The HTC ratio is used to depict the film influence on the HTC in comparison with the HTC without film cooling. It is essentially the dimensionless heat transfer coefficient, and the HTC ratio H is defined as:

$$H = \frac{h}{h_0} = \frac{T_{\infty 0} - T_{w 0}}{T_\infty - T_w} . \quad (4)$$

Uncertainty Analysis

Potential errors of experiment measurement come from two aspects. The first is the bottom plate is made of conductive material. It has a low thermal conductivity of 0.17W /m/K and was covered by another fiberglass pad with 0.04 W /m/K in the experiment. The comparing analysis of conjugate heat transfer simulation result to computational fluid simulation result has confirmed the film cooling effectiveness discrepancy due to conductivity(0.2) is less than 5%, which is considered the discrepancy caused by bottom wall conduction. In the HTC measurement, the heater foil is back-covered by a 10mm fiberglass pad and top-covered by a 0.2mm copper sheet to provide a uniform heat flux over the surface. The lateral conduction of the thin-foil heater is ignored (O'Dowd, 2009).

The other error sources come from measuring devices. Three major measuring uncertainties arise in the temperatures of mainstream， coolant and the cooled wall. The K-type thermocouple measures the mainstream and jet having an uncertainty of $\Delta Tc=\Delta T\infty=\pm 0.5$℃ after calibration. The maximum uncertainty of the IR camera is $\Delta Tw=\pm 0.5$℃ after calibration. The relative FCE uncertainty is 6.08%, and the H uncertainty is 5.56%. Final experimental uncertainties in the H and FCE measurements have been evaluated by the error propagation formula (Moffat,1982).

$$d\eta_{ad} = [(\delta_{\lambda})^2 + (\frac{\partial \eta_{ad}}{\partial T_{\infty}} dT_{\infty})^2 + (\frac{\partial \eta_{ad}}{\partial T_c} dT_c)^2 + (\frac{\partial \eta_{ad}}{\partial T_w} dT_w)^2]^{1/2} \cdot \quad (5)$$

$$dH = [(\frac{\partial H}{\partial T_{\infty 0}} dT_{\infty 0})^2 + (\frac{\partial H}{\partial T_{\infty}} dT_{\infty})^2 + (\frac{\partial H}{\partial T_{w0}} dT_{w0})^2 + (\frac{\partial H}{\partial T_w} dT_w)^2]^{1/2} . \quad (6)$$

RESULTS AND DISCUSSION

Film Cooling Effectiveness

Fig. 4 shows the contours of FCE distribution for the normal clean hole and three blocked holes under blowing ratio BR=1.0, 1.5, 2.0. The direction of crossflow is in the positive direction of Y. For the clean hole, the film effectiveness was slightly skewed asymmetric to one side opposite to the crossflow inflow direction (Y<0). In contrast, the film coverage was lateral symmetric when the coolant was fed by a plenum (Bonanni,2010). The coolant's crossflow produces a swirling flow at the hole entrance and destroys the symmetric flow in the diffuser.

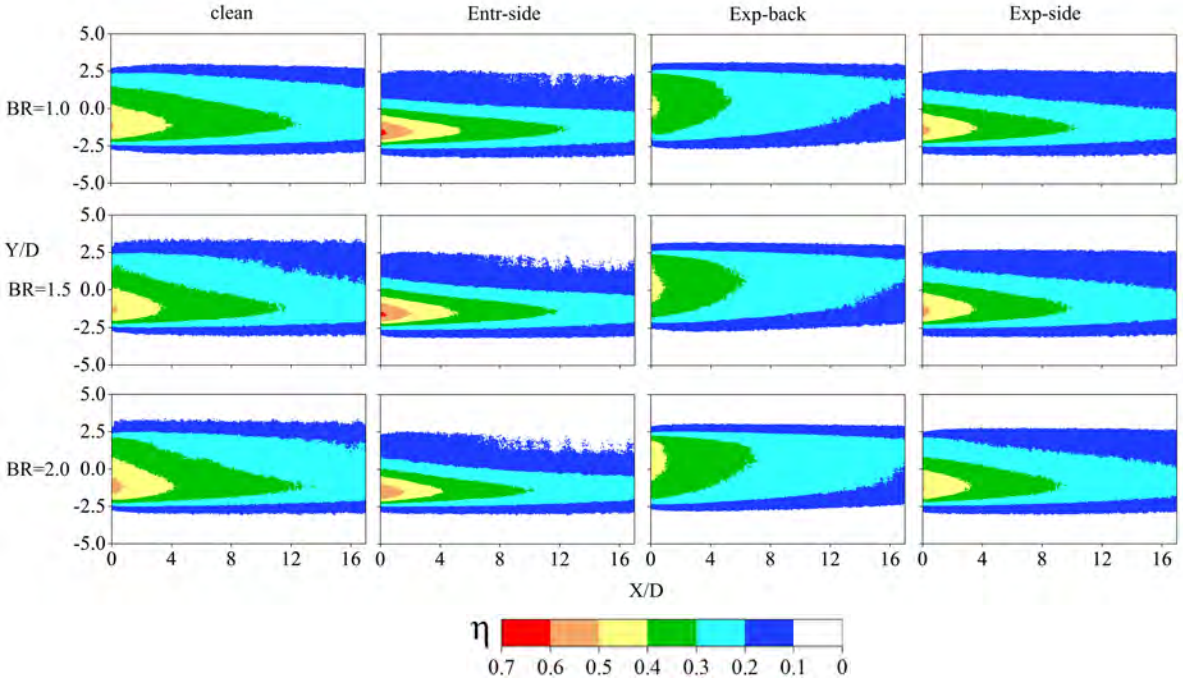

Figure 4 FCE distribution contour

For the Entr-side blocked hole, the blockage increases the magnitude of jet biasing. Its film coverage is smaller and more skewed to the lateral side comparing the clean hole. However, the maximum FCE value is higher than that of the clean hole, and the area of FCE higher than 0.5 of the Entr-side blocked hole is significantly larger than that of the clean hole.

For Exp-back blocked hole, the blockage decreases the magnitude of jet biasing and change skewness direction. Its skewed degree of film cover is low, and the distribution of FCE in the lateral direction becomes relatively uniform. However, the peak value of FCE is lowed. It is evident from the contour that the maximum FCE value is lower than 0.5. And the FCE skewed direction of the far-field is opposite to that of the clean hole, to be crossflow direction.

For the Exp-side blocked hole, the blockage increases the magnitude of jet biasing also. Comparing the result of the Exp-side blocked hole, its jets are biasing similarly, but at a lower magnitude.

The distribution shape of FCE of the four holes is similar for the BR varying among 1.0, 1.5, 2.0. It can be considered that the influence of blockage position on the distribution of the film is greater than that of blowing ratio. The distribution law of the FCE shows a great difference for four test film holes. This behavior indicated that the flow development in the holes was notably different due to the different blocking locations and therefore had significantly different flow structures as coolant left the holes (Saumweber, 2008; McClintic,2015b; Xu,2020).

Fig. 5 Comparing the lateral distribution of FCE for BR=1.0 at different downstream locations of the four holes. It can be seen that the FCE distribution was skewed for four holes. The direction and degree of the skewness are different. The local FCE values on the minus Y side are significantly higher than those on the other side for clean, Entr-side, Exp-side blocked holes. This effect is still visible in the far-field downstream area. Fig. 5 a comparing the lateral FCE distribution at X=1D of the four holes. It can be seen that the peak FCE values of Entr-side and Exp-side blocked holes are 0.61 and 0.52 respectively, which are higher than 0.50 corresponding clean hole condition. Both blockages have a larger effect of

distortion, hence lowers the FCE values on the positive Y side. Specifically, the cooling effectiveness decreases rapidly along with the pitch. The lateral distribution of the Exp-back blocked hole is relatively flat. Since the overall stability is balanced, the peak value of cooling efficiency is relatively low for only 0.42. Fig. 5 b and c comparing the lateral FCE distribution at X=9D and X=17D of the four holes respectively. It can be seen that the blockage advantage of high peak value is lost and the disadvantage of distortion is maintained for Entr-side, Exp-side blocked hole. Specifically, the peak value of Entr-side and Exp-side blocked holes gain advantage to clean hole at location X=9D even behind the clean hole at X=17D. But, the distortion of FCE is still significant downstream, which reduces the film cooling effect.

Fig. 6 compares the lateral averaged FCE of the four holes along the mainstream direction for BR=1. The FCE dissipation rate of Exp-back blocked hole condition is faster than in other cases. Specifically, the FCE values of the EXP-back blocked hole are the highest among the four holes at the position 1D after the exit of the hole, but it falls behind the other three holes after 11D, the FCE reduction is gradually increased along the mainstream direction. It can be concluded that the overexpanded cooling is of low intensity and difficult to maintain in the mainstream. The Entr-side and the Exp-back blocked holes meet a lower FCE value at the position 1D after the exit of the hole, and the value of backwardness remained unchanged along the mainstream direction.

Fig. 7 compares the variation of the area-averaged film cooling effectiveness of the four holes at blowing ratios varying to 1.0, 1.5, and 2.0. As a general expectation, the clean hole has the highest FCE values over tested blowing ratios, followed by Exp-back and Exp-side blocked holes, and the lowest is the Entr-side blocked hole. It is also found that the FCE values of the Entr-side blocked hole decrease at a higher blowing ratio while other holes get increased. This phenomenon is often seen in the results of circular gas film holes. The jet flow penetrating the mainstream at high blowing ratio, then the FCE decreases (McClintic,2015a). The Entr-side blockage concentrating the jet in the minus Y side of the hole exit to enter the mainstream at a very high velocity, shown intolerance to high blowing ratios.

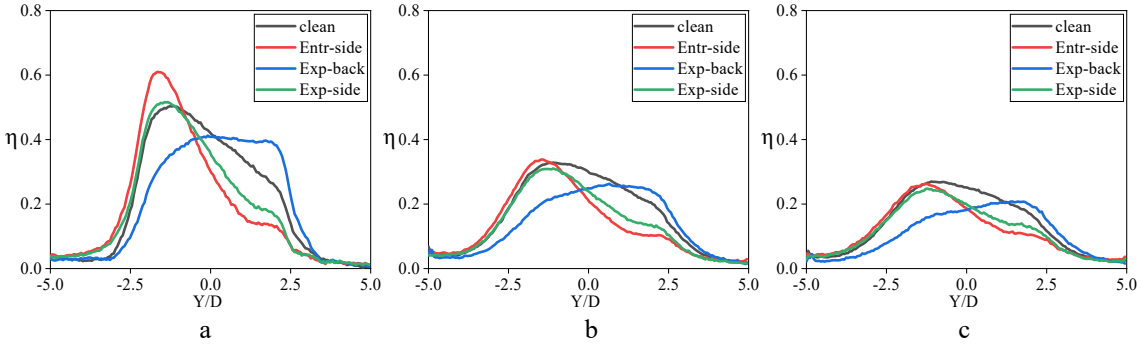

Figure 5 Lateral FCE distribution of BR=1.0 at location X=1D(a) X=9D(b) X=17D(c)

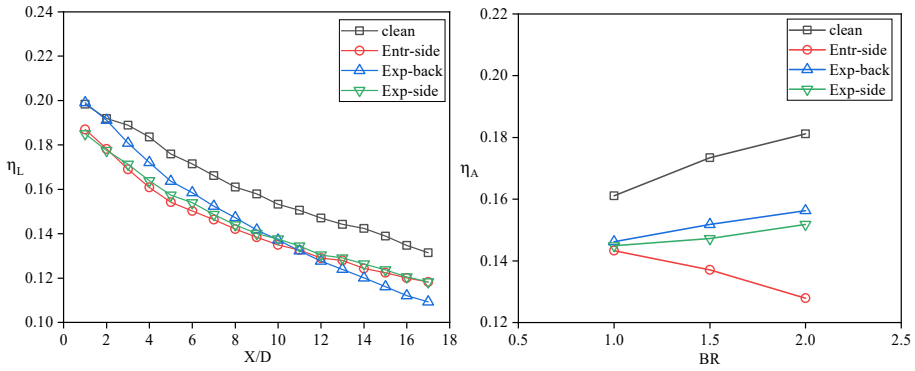

Figure 6 Lateral average FCE for BR=1.0 **Figure 7 Area average FCE diagram**

Heat Transfer Coefficient

Fig. 8 shows the contours of H distribution for the clean hole and three blocked holes to demonstrate the heat exchange performance. For the operation condition of all 4 holes and 3 blowing ratios, the high H value occurred immediately downstream of the holes, and the location of the highest heat transfer coefficient ratio was corresponding to the highest FCE position in the FCE contour. The H decrease as X increase, and it goes down at both ends in the Y direction. The results suggest that the film jets have strengthened on the wall heat transfer coefficient, and this strengthening amount depends on the strength of the jet and the distance from the center of the jet. The H of Entr-side blocked holes at the outlet of the hole is much higher than that of other cases. It means that the high exit momentum of Entr-side blockage can lead to a high heat transfer coefficient.

Fig. 9 shows the variation of HTC along the streamwise direction at blowing ratio BR=1 and the variation of area average HTC for different BR. Fig. 9 a showed that the Exp-back and Entr-side blocked holes raise an H higher than that of the clean hole to destroys the cooling conditions downstream of the hole. While Exp-side blocked hole gets the lowest H means lower heat transfer between the metal surface and mainstream. The H of Entr-side blocked holes is the highest for X⩽3D, but this advantage is only temporary. The H of Entr-side blocked holes drops rapidly indicate that the high heat transfer coefficient caused by high momentum jets has poor retainability. Fig. 9 b showed that the H advantage of cases Exp-back and Entr-side are maintained with the BR vary from 1 to 2, the backward of Exp-side blocked hole is maintained also. The heat transfer coefficient ratio of all holes increases with the increase of the blowing ratio. It can be considered that the efflux flow rate is an important factor affecting HTC.

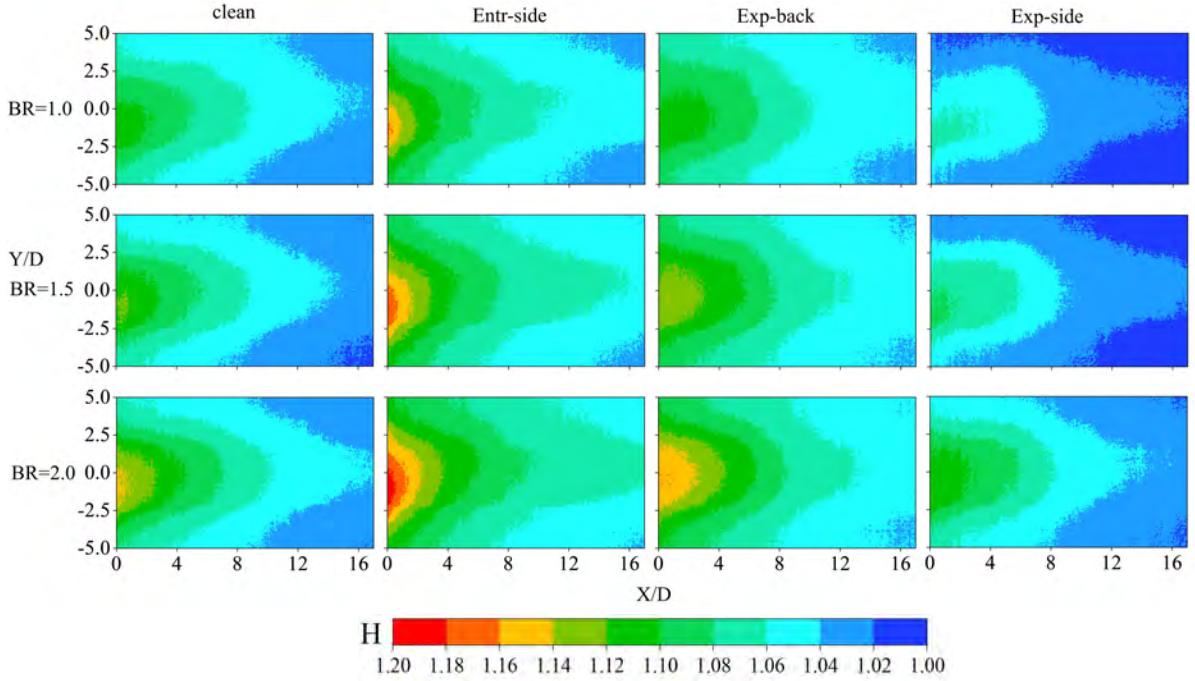

Figure 8 HTC ratio distribution contour for BR=1.0

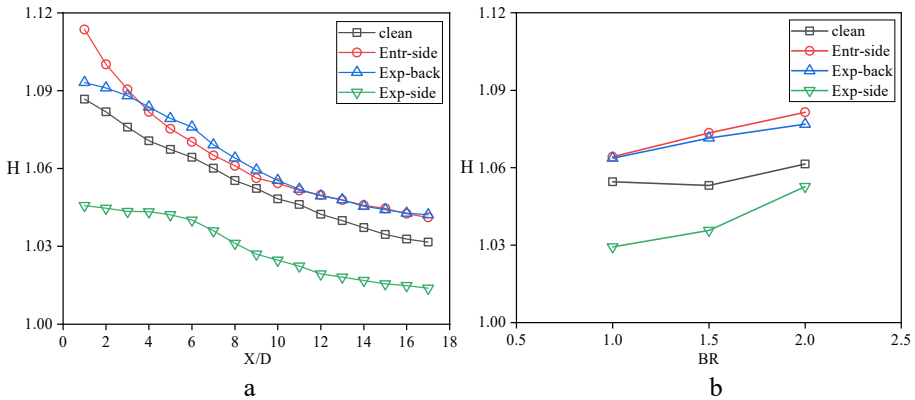

Figure 9 Lateral average H(a) and area average H(b)

DISCUSSION

Fan-shaped holes are often regarded as excellent shaped-hole. Fan-shaped holes have good FCE distribution under the condition of plenum coolant fed because of its advantages. The expansion part diffuses coolant at the lateral direction and slows down jet velocity, forming a very good lateral cooling effect and avoiding jet to penetrate the mainstream (Bunker,2005). But FCE value of fan-shaped holes is reduced under the crossflow condition (Saumweber,2008). The cooling effectiveness anomaly caused by the Exp-side blockage is the result of the combined influences of crossflow and blocking. The crossflow concentrates the jet at the minus Y side, which reduces the deceleration effect of the fan-shaped hole on the jet. The Entr-side blockage intensifies the concentrating effect, causing the jet in the minus Y side of the hole exit to enter the mainstream at a very high velocity. Although Entr-side gets a high peak FCE value, a lowest area average value, and the FCE decreases with the BR increase. The high jet outlet velocity of the Entr-side blocked hole makes the

heat transfer coefficient downstream of the hole very high, making the heat transfer coefficient of this hole become the highest. It means the Entr-side blocked hole is the worst performing in both HTC and FCE. The FCE distribution of Exp-side and Entr-side blocked holes are similar but H is completely different. The H of Entr-side is the highest and that of Exp-side is the lowest. So the effect of the two blockages cannot be considered to be the same type. More research is needed to understand the mechanism of this phenomenon.

CONCLUSIONS

Adiabatic effectiveness and heat transfer were measured for a fan-shaped hole fed by a crossflow channel. Three different pyramid elements were assumed to block the coolant flow at three positions respectively. Measurement covered the blowing ratio from BR=1.0 to 2.0. While both the effects of internal crossflow and blockage have been studied before, it is the first time to show the effect of blockage on a shaped hole fed by a crossflow channel.

Adiabatic effectiveness measured verifies that the blockage deduces the cooling performance including both the lateral averaged and area-averaged effectiveness values. The reduction amount varies according to the blockage locations, among which the blockage in the inlet round pipe caused the most serious reduction of 29.43% for BR=2.0. A possible explanation for this result is that the effective circulation area is reduced and thus increased the jet momentum. In addition, the blockage may intensify or dispel the skewed velocity profile due to the crossflow effect depending on its location.

The heat transfer coefficient is also measured to show the diversity of blockage effects on heat transfer. Blockages in the round pipe and diffuser laidback walls increased the heat transfer coefficient compared to no blockage condition, but the blockage on the diffuser side wall reduced the heat transfer coefficient compared to no blockage condition. Blockage in the holes significantly changes the heat transfer coefficient. The heat transfer coefficient ratio of all holes increases with the increase of the blowing ratio. It can be considered that the efflux flow rate is an important factor affecting the film cooling effectiveness.

Limited blockage cases have been measured in this paper and revealed complex effects on the film cooling performance. Further investigation is necessary to explain the relationships with crossflow direction as well as crossflow momentum.

NOMENCLATURE

Letter

BR:	Blowing ratio
D:	The diameter of the cylindrical segment of the hole
η:	Film cooling effectiveness
m	mass flow rate
h	Heat transfer coefficient
H	Heat transfer coefficient augmentation ratio
T	Temperature
U	Velocity
ρ	density
δ	discrepancy
X, Y	Cartesian coordinates

Subscript

ad:	Adiabatic wall
L:	Lateral average
A:	Area average
in	Crossflow inlet
out	Crossflow outlet
h:	Hole
c:	Coolant
∞:	Mainstream
0	No film cooling
λ	heat conduction

ACKNOWLEDGMENTS

This study is partly supported by the National Science and Technology Major Project under contract No. 2017-V-006-0069.

REFERENCES

Bonanni, L., Facchini, B., Tarchi, L., Maritano, M.,Traverso, S. (2008) .Heat Transfer Performance of Fan-Shaped Film Cooling Holes: Part I—Experimental Analysis. Proceedings of the ASME Turbo Expo 2010: Power for Land, Sea, and Air. Glasgow, UK. pp. 1561-1571. Available at:https://doi.org/10.1115/GT2010-22808.

Bunker, R. (2000).Effect of Partial Coating Blockage on Film Cooling Effectiveness.In: Proceedings of the ASME Turbo Expo 2000: Power for Land, Sea, and Air. [online] Munich, Germany. V003T01A051. Available at: https://doi.org/10.1115/2000-GT-0244.

Bunker, R. (2005). A review of shaped hole turbine Film-Cooling technology. Journal of Heat Transfer, 127(4)pp. 441-453.

Chen, X. , Wang, Y. , Long, Y. , Weng, S.(2021). Effect of partial blockage on flow and heat transfer of film cooling with cylindrical and fan-shaped holes. International Journal of Thermal Sciences, 164,106866. Available at: https://doi.org/10.1016/j.ijthermalsci.2021.106866.

Goldstein, R. J., Taylor, J. R. (1982). Mass Transfer in the Neighborhood of Jets Entering a Crossflow. Journal of Heat Transfer, 104(4), 715-721. Available at: https://doi.org/10.1115/1.3245190.

Huang, K ., Zhang, J ., Tan, X . (2018).Experimental study on film cooling performance of imperfect holes. Chinese Journal of Aeronautics,31(6), pp.1215-1221.

Jovanovic, M.B., Lange ,H ., Steenhoven ,A .(2008). Effect of hole imperfection on adiabatic film cooling effectiveness.International Journal of Heat and Fluid Flow, 29(2), pp.377-386.

Kohli, A., Thole, K.A., (1998).Entrance Effects on Diffused Film-Cooling Holes. Proceedings of the ASME 1998 International Gas Turbine and Aeroengine Congress and Exhibition. Stockholm, Sweden. V004T09A070. Available at: https://doi.org/10.1115/98-GT-402.

Lee, S., Hwang, W., Yee, K. (2018). Robust design optimization of a turbine blade film cooling hole affected by roughness and blockage. International Journal of Thermal Sciences, 133, pp.216-229.

McClintic, J., Klavetter, S., Winka, J, Anderson, J., Bogard, D., Dees, J., Laskowski, G., and Briggs, R. (2015). The Effect of Internal Crossflow on the Adiabatic Effectiveness of Compound Angle Film Cooling Holes. Journal of Turbomachinery, 137(7): 071006. Available at: https://doi.org/10.1115/1.4029157.

McClintic, J., Wilkes, E., Bogard, D., Dees, J., Laskowski, G., Briggs, R. (2015).Near-Hole Thermal Field Measurements for Round Compound Angle Film Cooling Holes Fed by Cross-Flow.In: Proceedings of the ASME Turbo Expo 2015: Turbine Technical Conference and Exposition. Montreal, Quebec, Canada. V05BT12A050. Available at: https://doi.org/10.1115/GT2015-43949.

Moffat, R. J.(1982). Contributions to the theory of single-sample uncertainty analysis. Journal of Fluids Engineering, 104(2), 250--260. Available at: http://dx.doi.org/10.1115/1.3241818.

O'Dowd, D., Zhang, Q., Ligrani, P ., He, L., and Friedrichs, S. (2009). Comparisons of Heat Transfer Measurement Techniques on a Transonic Turbine Blade Tip. ASME Paper No. GT2009-59376. Available at: https://doi.org/10.1115/GT2009-59376

Saumweber, C., Schulz, A. (2008).Comparison the Cooling Performance of Cylindrical and Fan-Shaped Cooling Holes With Special Emphasis on the Effect of Internal Coolant Cross-Flow. Proceedings of the ASME Turbo Expo 2008: Power for Land, Sea, and Air. Berlin, [online]Germany. pp. 893-903. Available at: https://doi.org/10.1115/GT2008-51036.

Walsh, W. S., Thole, K. A., Joe, C.(2006).Effects of Sand Ingestion on the Blockage of Film-Cooling Holes. In: Proceedings of the ASME Turbo Expo 2006: Power for Land, Sea, and Air.[online] Barcelona Spain, pp. 81-90. Available at:https://doi.org/10.1115/GT2006-90067

Wilkes, E., Anderson, J., McClintic, J., & Bogard, D. (2008).An Investigation of Turbine Film Cooling Effectiveness With Shaped Holes and Internal Cross-Flow With Varying Operational Parameters.Proceedings of the ASME Turbo Expo 2016: Turbomachinery Technical Conference and Exposition. Seoul, South Korea. V05CT19A004. Available at: https://doi.org/10.1115/GT2016-56162.

Xu, G., An, B., Yu, Z., Li, C. (2020).Numerical investigation on film cooling characteristics of slot-sectional diffusion holes combined with an internal cross-flow channel, Applied Thermal Engineering, 181,115953. Available at:https://doi.org/10.1016/j.applthermaleng.2020.115953.